Experimental test of the birdsong error-correction model

Anthony Leonardo*

Computation and Neural Systems Program, California Institute of Technology, Pasadena, CA 91125

Communicated by Masakazu Konishi, California Institute of Technology, Pasadena, CA, October 22, 2004 (received for review September 12, 2004)

Adult zebra finches require auditory feedback to maintain their songs. It has been proposed that the lateral magnocellular nucleus of the anterior nidopallium (LMAN) mediates song plasticity based on auditory feedback. In this model, neurons in LMAN, tuned to the spectral and temporal properties of the bird's own song (BOS), are thought to compute the difference between the auditory feedback from the bird's vocalizations and an internal song template. This error-correction signal is then used to initiate changes in the motor system that make future vocalizations a better match to the song template. This model was tested by recording from single LMAN neurons while manipulating the auditory feedback heard by singing birds. In contrast to the model predictions, LMAN spike patterns are insensitive to manipulations of auditory feedback. These results suggest that BOS tuning in LMAN is not used for error detection and constrain the nature of any error signal from LMAN to the motor system. Finally, LMAN neurons produce spikes locked precisely to the bird's song, independent of the auditory feedback heard by the bird. This finding suggests that a large portion of the input to this nucleus is from the motor control signals that generate the song rather than from auditory feedback.

auditory feedback | behavior | lateral magnocellular nucleus of the anterior nidopallium | single neuron | songbird

Error correction, based on sensory feedback, plays a critical role in many biological systems. Humans must hear themselves to speak normally. Manipulations of auditory feedback reveal that we change our pronunciation of words, virtually in real time, if they do not sound correct. These changes are adaptive and reduce the perceived error in speech (1). Like humans, songbirds must hear themselves to sing properly. Auditory feedback is required by songbirds both to learn a tutor song (2) and to maintain the stable structure of their "crystallized" adult songs (3–5). The brain nuclei of the song control system (6) afford a unique opportunity to explore the neural basis of an error-correction signal that is required to learn and produce complex vocalizations.

Abundant experimental evidence has linked the lateral magnocellular nucleus of the anterior nidopallium (LMAN) (6–8) with the processing of auditory feedback and song error correction. Manipulations of LMAN in juvenile songbirds interfere with the memorization of the tutor song that the bird uses as a template to shape his own vocalizations (9, 10). Furthermore, lesions to LMAN in adult birds block deafening-induced changes to song (11). These results, and the anatomy of the song control system, have led to the hypothesis (12) that an error signal, based on auditory feedback, is sent from LMAN to the robust nucleus of the arcopallium (RA) (6, 8) (Fig. 1). This error signal is presumed to initiate changes in the song motor program such that future vocalizations are a better match to the song template.

The two major models of birdsong plasticity differ in the manner in which they use auditory feedback for error correction. The bird's own song (BOS)-tuned model (Fig. 1*b*) proposes that auditory feedback is used directly for error correction in real time as the bird is singing (11). The BOS-tuned model is based on the observation that LMAN neurons in the anesthetized bird are song-selective: they are precisely tuned to the spectral and temporal properties of the individual BOS (13). When a BOS-tuned neuron in an anesthetized bird is presented with playback of the BOS, it responds with a dramatic increase in firing rate. Other acoustic stimuli, such as white noise (WN), produce little or no changes in firing rate (14). This property develops over the course of song learning; interference with the learning process produces birds that copy the tutor song poorly and have a concurrent loss of tuning to the BOS (15). The BOS-tuned model postulates that song-selective LMAN neurons act as error detectors, directly comparing the bird's vocalizations to the song

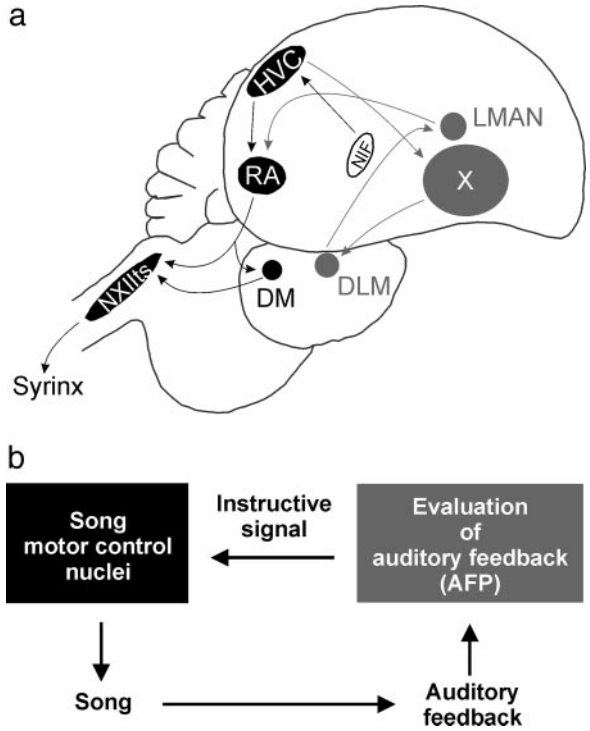

Fig. 1. Anatomy of the song control system and proposed error-correction model. (*a*) The processes of song motor control and song learning form the two major pathways between a set of discrete brain nuclei known collectively as the song system (6). The projection from LMAN to RA links the anterior forebrain pathway (gray) associated with song plasticity to the motor control pathway (black) associated with song production. (*b*) BOS-tuned error-correction model schematic, adapted from Brainard and Doupe (11). Song motor control nuclei generate the bird's song. Auditory feedback from the song is evaluated in the anterior forebrain pathway and compared to the song template via neurons tuned to the bird's song. LMAN, the output of the anterior forebrain pathway, sends the error signal to the premotor nucleus RA.

Abbreviations: LMAN, lateral magnocellular nucleus of the anterior nidopallium; BOS, bird's own song; RA, robust nucleus of the arcopallium; WN, white noise; ISI, interspike interval.

*Present address: Department of Molecular and Cellular Biology, Harvard University, Cambridge, MA 02138. E-mail: leonardo@fas.harvard.edu.

template and relaying this instructive signal to the motor control system (12, 14, 16).

In contrast to the BOS-tuned model, the efference copy models use auditory feedback indirectly for error correction. In these models, the bird learns to predict the auditory feedback that should result from each set of motor commands. The prediction of expected auditory feedback is then used for error correction (via the LMAN pathway) either during singing (17) or when the bird is asleep (18, 19). Error correction within the efference copy model could occur more quickly than in the BOS-tuned model because one does not have to wait for the arrival of auditory feedback (an ≈50-ms delay) (17).

The experiments in the present study test both the BOS-tuned and efference copy models of error correction by measuring the firing properties of single LMAN neurons while simultaneously manipulating the auditory feedback heard by singing birds. A direct prediction of the BOS-tuned model is that, during singing, the activity of LMAN neurons will depend on the match between the auditory feedback from the bird's song and the memorized song template. In contrast, the efference copy model predicts that, rather than auditory feedback, LMAN is largely driven by the motor signal used to generate the song (and the prediction of expected auditory feedback), and, therefore, LMAN spike patterns should be locked to the bird's song yet insensitive to changes in auditory feedback.

Computer-controlled perturbation of auditory feedback during song production presents a way to explore the dynamics of the song error-correction process that is not possible with deafening. Auditory feedback perturbation causes the crystallized song to deteriorate over a period of weeks into a large number of highly variable songs; the result of this process is termed "decrystallization" (Fig. 2*a*). Restoration of normal auditory feedback allows the recovery of the original song and reveals that song stability is an active process (20). However, changes in LMAN activity during song production in a decrystallized bird would be difficult to interpret; they could occur either because the bird hears different auditory feedback or because the bird sings differently. This confound would make it difficult to discriminate between the BOS-tuned and efference copy models of error correction, which postulate the LMAN neurons are driven by an auditory feedback or motor signal, respectively. Therefore, in the current study I investigated error correction in birds with stable songs; the error-correction signal must still be present in order for decrystallization to occur later, and, because song structure does not change, any changes in the activation of LMAN neurons must be solely caused by the auditory feedback perturbation.

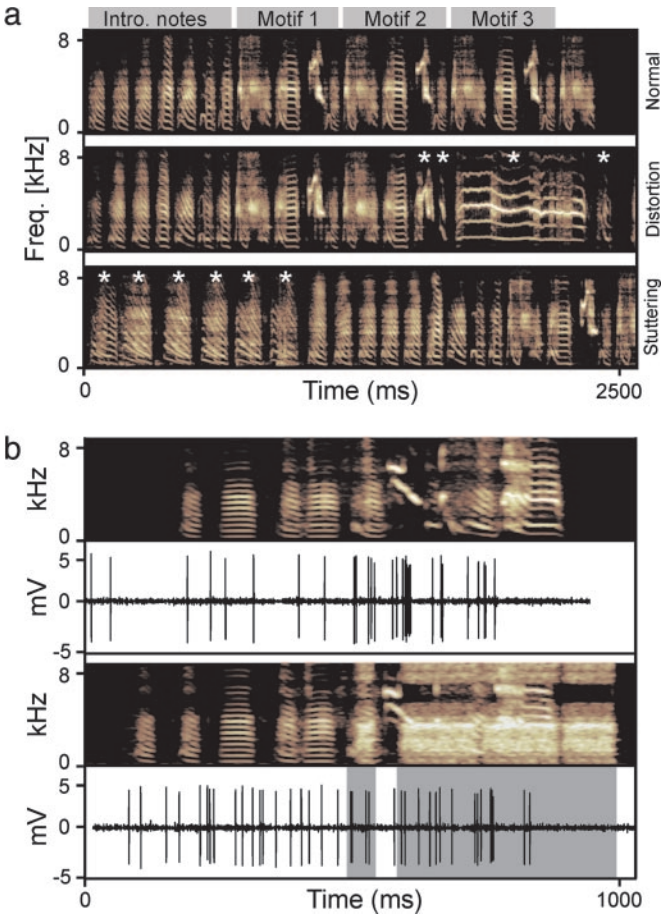

Fig. 2. The effects of altered auditory feedback on zebra finch song and LMAN neural activity. (*a*) Altered auditory feedback causes stable song structure to deteriorate. (*Top*) Normal song of bird d7, showing introductory notes and the repeated song motif, composed of stereotyped syllables. After 1 month of continuous WN feedback, the bird produced songs with new and distorted syllables (*Middle*, white asterisks), and songs with stuttered syllables (*Bottom*, white asterisks). (*b*) Single-neuron recordings in LMAN were made in birds singing stable songs but hearing both normal (*Top*) and altered (*Bottom*) auditory feedback (neuron b7c28). Modulated WN masks half of the song in the bottom panel (gray background). The 1.5-kHz notch in the noise spectrum was used by the computer to continuously detect when the bird was singing.

Materials and Methods

Zebra finches (*Taeniopygia guttata*) were housed individually in custom-designed Plexiglas cages and had unlimited access to food and water. Animal care was in accordance with California Institute of Technology and National Institutes of Health guidelines. All of the birds used in the study were young adults (≈120 days old) with crystallized songs; previous work has shown that younger birds tend to have higher song plasticity than older birds (21). After baseline song data were collected for 1 week, each bird was anesthetized with 1–2% isoflurane and a miniature motorized microdrive was implanted above nucleus LMAN based on stereotaxic coordinates and physiological activity (22). The microdrive weighs ≈1 g and contains three independently controlled motors, allowing each electrode to be positioned extracellularly with 0.5-μm resolution. Electrodes were made from 80-μm tungsten wire, insulated with parylene, and had ≈3-MΩ impedance (Microprobe, Gaithersburg, MD).

Experimental Design. It has been shown that the pattern of multiunit activity present in LMAN during song production remains essentially unchanged after deafening (23). However, Hessler and Doupe (23) compared different multiunit sites before and after deafening. In this study I focused on single LMAN neurons and recorded the spiking output of each neuron during singing with both normal and altered auditory feedback. Individual LMAN neurons were isolated in the awake, nonsinging bird. BOS-tuned neurons in LMAN are known to be projection neurons that leave LMAN and make synapses onto premotor neurons in RA (16). These neurons are expected to carry the error signal. LMAN also contains interneurons, whose role in error correction is less clear. However, intracellular studies have shown that it is difficult to record from LMAN interneurons (24), and there are no reports of interneurons' being recorded extracellularly to date. The LMAN neurons described in this study were a homogeneous population, and their large spike amplitudes (1–15 mV) are consistent with their being projection neurons (24), making it unlikely that any interneurons were sampled.

Once a neuron was well isolated, a female bird was presented to elicit directed singing (25) with normal and altered auditory feedback (Fig. 2*b*). Upon conclusion of the experiment (≈1 week

of recordings), electrolytic lesions were made in LMAN by passing −3 μA of current through each electrode for 10 s (three times). The bird was then killed with an overdose of isoflurane, and the brain was recovered and fixed overnight in 3% paraformaldehyde. The following day, the brain was sliced into 100-μm sections on a vibratome, and the lesions were verified to be in LMAN.

Computer-Controlled Perturbation of Auditory Feedback. During each experiment, a computer monitored the bird's vocalizations in real time (20), detected singing, and randomly allowed the birds to sing either normally or with altered auditory feedback (Fig. 2*b*). The altered auditory feedback signal was played through a speaker mounted on one wall of the cage and was recorded with an omnidirectional microphone mounted on a perpendicular cage wall. The amplitude of the artificial auditory feedback was calibrated to be equal to or greater than the bird's own vocalizations (≥95 dB) upon reaching the bird's ear. This calibration was approximate because the bird moved freely within its cage. The computer continuously acquired 50-ms segments of sound from the microphone (40-kHz sampling rate). Each of these bins of sound was passed through a software-based infinite impulse response filter (≈5.5- to 7.0-kHz bandwidth, but this varied slightly from bird to bird to optimize triggering accuracy). If the rms amplitude of the filtered signal exceeded a threshold, artificial auditory feedback was triggered by the computer. Custom-designed software, written in LABVIEW (National Instruments, Austin, TX), was used to control all aspects of the experiment.

WN Feedback. WN was continuously generated from a random distribution and was modulated with a 7-Hz envelope (the approximate periodicity of the song syllables forming a motif). This signal was then passed through a second infinite impulse response filter with a 1.5-kHz notch in the location of the sound bandwidth used for song detection (Fig. 2*b*). The bandwidths of the song-detection signal and the auditory feedback perturbation signal were completely decoupled, preventing a positive-feedback loop between the speaker and the microphone and allowing the entire song to be covered with altered feedback.

Previously, a delayed auditory feedback protocol (20) has been used to cause the bird to hear his own song superimposed with a delayed copy of the song. This protocol alternated detecting singing and producing altered feedback to avoid a positive feedback between the speaker and microphone. A consequence of this procedure is that very different superpositions of normal and altered feedback occur each time the bird sings, and only 30% of the song is covered with altered feedback, complicating averaging the neural activity across different song repetitions. In contrast to the delayed-syllable procedure, the WN protocol allows the spectrum of sound heard by the bird to be changed much more dramatically, masks the bird's vocalizations in approximately the same manner each time, and covers 100% of the song with feedback. These properties allow more reliable estimation of the average neural response to the altered feedback stimulation. Therefore, in this study, WN was chosen as the altered-feedback stimulus because it seemed more likely than delayed auditory feedback to reveal an error signal in the LMAN activity.

WN feedback was not applied long enough to produce song decrystallization, because of the reasons discussed in the Introduction, but it was important that it be known to be an effective feedback stimulus. Although the birds never received altered feedback in the 5.5- to 7.0-kHz band used to detect singing, prior studies in Bengalese finches have shown that high-frequency sound is not sufficient for song maintenance (26). More importantly, the WN-feedback protocol was verified to cause song decrystallization in a separate bird (Fig. 2*a*). Other studies (27) have also used WN feedback to elicit changes in the learned songs of adult zebra finches.

Active Sound Cancellation. The randomization of normal- and altered-feedback singing was designed such that no decrystallization of the bird's song would occur during the experiment. In addition to this design, further precautions were taken to ensure the songs remained stable. Because the microphone recorded the superposition of the altered feedback and the bird's vocalizations, direct inspection of the recordings for song stability was not possible. An active sound cancellation system was used to measure the transfer function of the acoustic environment (speaker, cage, bird, microphone) and predict what the altered feedback from the speaker would look like at the microphone. This prediction could later be subtracted from the microphone signal, leaving only the bird's vocalizations. However, the bird was constantly moving, making the transfer function of the acoustic environment highly nonstationary. It was not possible to simply calibrate the system at the start of the experiment and then use this single fixed transfer function for feedback prediction. This problem was solved by measuring the transfer function in real time, effectively taking a snapshot of the acoustic environment each time the bird sang.

The nonstationary transfer function of the acoustic environment was measured immediately after each song was produced, by using a Golay code pair (28, 29). Golay codes (30) are complementary series of binary numbers whose autocorrelation side lobes are inverses of each other such that their sum is a delta function. This property enables the measurement of a transfer function with an extremely short probe sequence. Each Golay code was 12.5 ms in length separated by a 12.5-ms silent interval, resulting in a 50-ms calibration signal. The sound cancellation system produced an ≈30-dB reduction in the amplitude of the altered feedback from the microphone signal. Each transfer function was used offline to cancel the altered feedback from the simultaneously recorded microphone signal and to verify that the altered feedback did not cause the birds to sing differently during the experiment (Fig. 3).

Data Analysis

Spectral Analysis. The time-frequency spectrogram for each song was calculated with an 8-ms window sliding in 0.5-ms steps, in which each time point consisted of the direct multitaper estimate (31) of the power spectrum. Spectral time derivatives used in the song alignment were estimated by using the methods described in ref. 32.

Song Alignment. The lengths of the individual syllables in zebra finch song vary independent of each other from song rendition to rendition by ≈1–5%. If the spike trains are aligned only to the onset of the bird's song, there is considerable noise in estimates of the neuron's average time-varying spike rate. However, the variability from this acoustic time warping can be removed by using spectral derivative peaks (32), which mark the onsets of song syllables, as reference points. These reference points were used to linearly stretch and compress common segments of sound (from different song recordings) to be the same length. See ref. 33 for additional technical details. This piecewise linear time warping is based on only the song and is completely independent of the spike trains. Each spike train was then projected onto the normalized time axis of its corresponding acoustic signal. The end result of this procedure is that all of the sequentially recorded spike trains are on a common song-aligned time axis and may now be compared directly with each other (Fig. 3). The plausibility of the linear stretching and compression operation for syllable alignment can be seen in prior studies (33) in which this procedure results in submillisecond alignment of spikes in nucleus RA. The active sound cancellation system

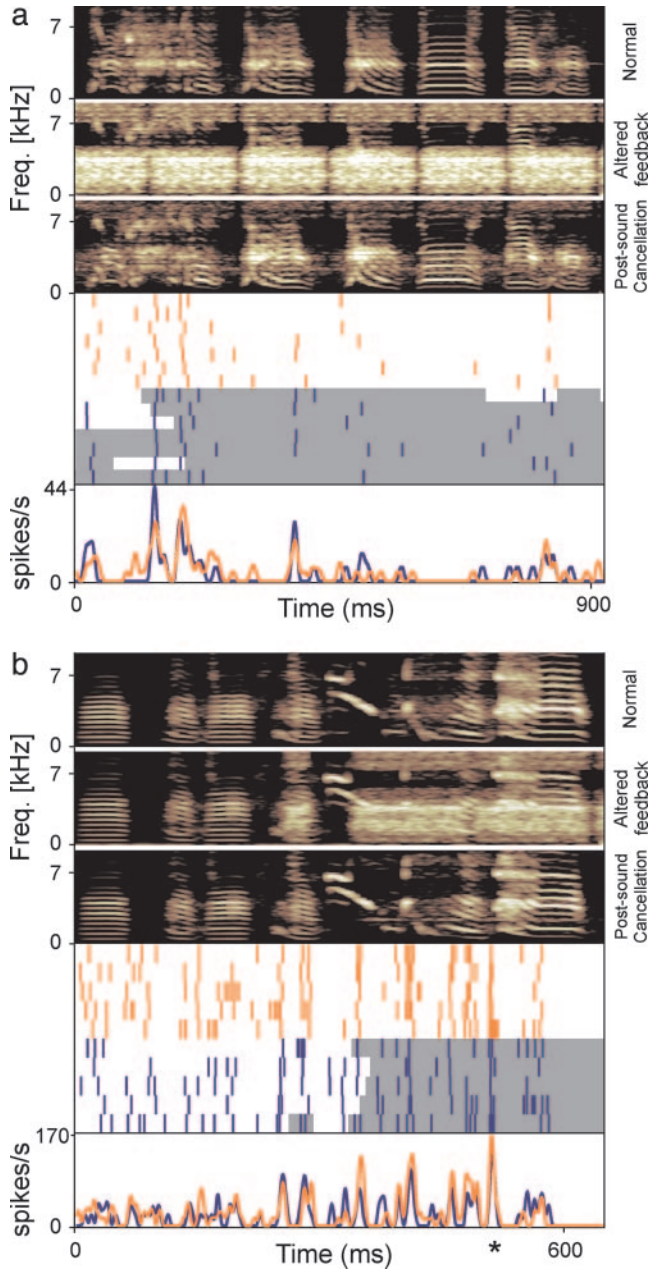

Fig. 3. Song-aligned LMAN spike patterns during singing with normal and altered auditory feedback. (*a*) The first row shows the song spectrogram for bird 8 during singing with normal auditory feedback. The second row shows a representative song spectrogram during singing with altered auditory feedback. The third row shows a representative song spectrogram during singing with altered auditory feedback after using the sound cancellation system to recover the bird's vocalization. Note that the spectral structure of the song syllables is virtually identical to that seen during normal auditory feedback (first row), in contrast to the decrystallization that occurs after prolonged altered-feedback exposure as shown in Fig. 2*a*. The fourth row shows spike rasters for neuron b8c8 during normal-feedback (orange) and altered-feedback (blue) singing. Gray bars show the temporal location of the altered feedback. The fifth row shows the average firing rate for neuron b8c8 during normal- and altered-feedback singing. (*b*) Same as in *a* for bird 7, neuron b7c28. The asterisk marks an exemplar burst of spikes that is locked precisely to structure in the bird's song during both normal- and altered-feedback singing.

discussed above is needed to align the songs produced during the altered-feedback singing (which are entirely masked with WN when initially recorded).

Spike Rate Analysis. In studies of BOS-tuning in anesthetized birds, it has become conventional to compare LMAN firing rates to different auditory stimuli using the d' statistic with a threshold criterion of 0.5 (34). d' measures the distance between two Gaussian distributions, normalized by their standard deviations; it is equivalent to a paired t test. However, the 0.5 d' criterion is based on a fixed sample size. In the current experiment, the bird produced different numbers of normal- and altered-feedback songs for each neuron. Because of this, the paired t test was used directly to compare LMAN spike rates during normal- and altered-feedback singing. Use of the t test allowed a constant level of statistical significance ($P < 0.01$) to be maintained despite the varying number of recorded songs for each neuron.

Interspike Interval (ISI) Analysis. The average ISI distribution for each neuron's spike pattern produced during normal- and altered-feedback singing conditions was estimated in the following manner. Each spike train recorded during normal singing was smoothed with a 10-ms Hanning window and averaged into a time-varying mean spike-rate estimate. The summed absolute difference was then calculated between each smoothed spike train and the time-varying mean rate. The spike train that had the smallest deviation from the time-varying mean rate was then selected as the representative spike train for the normal-feedback condition for that neuron, and the ISI distribution was calculated. A similar procedure was used with the spike trains generated during altered-feedback singing, resulting in a representative altered-feedback singing spike train and ISI distribution. By computing the ISI distribution from a single representative spike train for each neuron, I avoided the problem of the distributions' being skewed by outliers present in some of the small song sample sizes.

To avoid a bias from using exemplar ISI distributions rather than the entire data set, I computed the population ISI distribution for each feedback condition across all of the sampled neurons. For each feedback condition, the first four spike trains recorded from each neuron during that feedback condition were selected and added to a pooled ISI histogram.

Spike Precision Analysis. To calculate how precisely the spikes of each LMAN neuron were locked to acoustic structure in the bird's song, the following algorithm was used. For each time t in the song, the minimum window (w) was found such that the probability that neuron i fired a spike in the time range $t \pm w$ was $\geq$0.75 over all normal song spike trains recorded for that cell. This procedure generated a time-varying vector, in which each element of the vector indicated how precisely spikes were generated at that time in the song. The minimum of the vector was identified; this was the smallest time window in which a spike event reliably occurred. This time point and its width (the identified minimum) were stored, and the spikes they represented were removed from the original set of normal song spike trains. The removal of the most precise spike event produced minor changes in the membership of neighboring spike events. The precision vector was then recalculated, and the entire procedure (select minimum event, store, remove) was repeated until no further events were detected. The final list of stored events represents the distribution of precise events and their respective widths for the neuron during normal singing. The same procedure was repeated for the altered-feedback spike trains for that neuron. This method produced a distribution of spike event precisions that was relatively independent of the threshold probability used to identify the spike events. The spike precision was calculated only for neurons with at least four recorded motifs of normal- and altered-feedback song to ensure sufficient sample sizes for statistical analysis.

Results

LMAN Firing Rates During Singing with Normal and Altered Auditory Feedback. A total of 17 LMAN neurons were recorded in four zebra finches (Fig. 2*b*). The average spontaneous firing rate of LMAN neurons in the awake bird was 13.2 ± 7 (SD) spikes per second: An average of eight songs per neuron (range, 3–19) was recorded for singing with normal auditory feedback, and an average of six songs per neuron (range, 2–16) was recorded for singing with altered auditory feedback. The spike trains of each neuron were aligned across multiple renditions of the song, allowing an estimate of each neuron's average firing pattern (Fig. 3). During song production, LMAN neurons had sharp peaks in firing rate and produced 24.0 ± 12 (SD) spikes per second during singing with normal auditory feedback. The average LMAN firing rate during singing with altered auditory feedback was 23.7 ± 12 (SD) spikes per second. The average difference in LMAN neuron spike rates between normal- and altered-feedback singing, across the population of recorded neurons, was 0.3 ± 1 (SE) spikes per second and was not significantly different from zero ($P = 0.75$, t test). There were also no significant differences between the spike rates of individual LMAN neurons during singing with normal versus altered auditory feedback (paired t test, $P > 0.01$ for all neurons; average, $P = 0.27$).

LMAN ISI Distributions During Singing with Normal and Altered Auditory Feedback. To address whether there were changes in LMAN spike patterns concurrent with changes in auditory feedback that were not reflected in the mean firing rates, the ISI distributions between the normal- and altered-feedback spike trains were computed for each LMAN neuron. A consistent change in spike timing, such an increase in firing rate localized to a small portion of the song, would manifest itself as an increase in ISIs of a certain length. LMAN ISIs ranged from 4 to 56 ms (90% of distribution), with a median of 25.2 ms (normal singing). A Kolmogorov–Smirnoff test found no significant differences between the normal- and altered-feedback ISI distributions for any of the individual neurons ($P > 0.01$; average, $P = 0.54$) or for the population data pooled across all four birds ($P = 0.28$; Fig. 4*a*).

LMAN Spike Precision During Singing with Normal and Altered Auditory Feedback. If LMAN neurons respond to auditory feedback during singing, spike timing precision should change as the altered feedback masks spectral features in the normal auditory feedback of the bird's song. For each time t in the song, it was determined how large a window was needed such that there was a probability of at least 0.75 that the neuron would fire a spike within the time window. This partitioned the song into a series of spike events of varying widths; the distribution of these widths indicated how precisely each neuron generated its time-varying spike pattern. LMAN neurons produced 13 ± 7 (SD) spike events per song during normal- and altered-feedback singing ($P = 0.88$, Kolmogorov–Smirnoff test), with a median precision of 6 ms (range, 0.5–33 ms, 90%). No significant differences were found between the normal- and altered-feedback spike event width distributions for any of the neurons ($n = 12$ neurons; $P > 0.01$; average, $P = 0.87$, Kolmogorov–Smirnoff test; see Fig. 4*b*). Remarkably, 30% of the spike events generated by LMAN neurons had a precision of <2 ms, indicating that LMAN neurons produce spikes locked with millisecond precision to acoustic structure in the bird's song even when that acoustic structure was entirely masked by noise.

Discussion

LMAN activity in awake singing birds presents us with substantial differences from that seen in anesthetized studies. The firing rates of single LMAN neurons in the singing bird are nearly four times larger than those seen during song playback in the anesthetized bird [≈24 spikes per second vs. ≈6 spikes per second (14)]. Furthermore, based on a variety of statistical tests, the firing rates of LMAN neurons in the singing zebra finch are insensitive to changes in auditory feedback. The average difference in LMAN firing rates during singing with normal vs. altered auditory feedback was only 0.3 spikes per second and was not significantly different from zero. The minimum firing rate difference (35) detectable by the t test was 4.3 spikes per second. Because song motifs are generally <1 s in length, this finding constrains any song error-correction signal encoded by single LMAN neurons to be at most a change of two to three spikes per motif from the normal firing pattern.

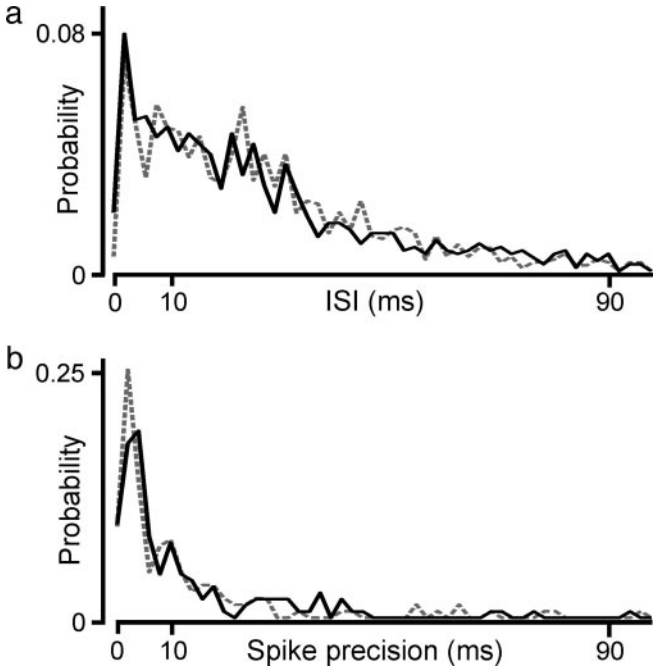

Fig. 4. Analysis of LMAN activity during singing with normal and altered auditory feedback. (*a*) ISI distributions for each singing condition, pooled across all neurons. (*b*) Spike precision distributions for each singing condition, pooled across all neurons. Probabilities were calculated in 2-ms bins.

The data presented in this paper are not consistent with the notion that BOS-tuned neurons in LMAN encode an error-correction signal based on auditory feedback and raise important questions about what role LMAN plays in song plasticity. It is possible that changes in the spike timing between LMAN neurons could encode the degree of mismatch between the bird's vocalizations and the song template, although there is currently no evidence for such a model. Alternatively, there may have been an unsampled subtype of LMAN projection neurons that encodes the error-correction signal based on firing rate modulations. However, such heterogeneity of LMAN cell types has not been seen in prior studies. Finally, it is known that the time course of changes in song structure from perturbation of auditory feedback is slow [on the order of weeks or months (3, 20)], suggesting that LMAN may relay the error signal to RA only after it exceeds some threshold for sufficient time. This revised model would move the computation of the error signal out of LMAN and to brain nuclei earlier in the song control system. However, all of these alternative models leave a critical observation unresolved: what is the function of the precise song-locked spike patterns generated in LMAN during singing?

The precise song-locked LMAN spike patterns persisted even when the altered auditory feedback prevented the bird from

hearing his own vocalizations. For example, the neuron in Fig. 3*b* fires a short burst of spikes at a time of 512 ms. These spikes are locked with millisecond precision to the bird's song. If this spike burst were driven by auditory feedback, one would expect it to become substantially less precise when the bird sang with altered feedback, because the acoustic structure of the song is masked with WN. However, if the burst were generated by the motor signals that drive song production, it would still be generated reliably during altered auditory feedback. The LMAN neurons in this study produced many spikes locked to the bird's song with a precision of <2 ms during singing with altered auditory feedback; this precision is similar to that seen in premotor neurons of the song control system (36). These data therefore provide the most direct evidence to date that, during song production, individual LMAN neurons are driven largely by a signal with a motor origin rather than an auditory one, as suggested previously (37, 38). A motor input to LMAN during singing is consistent with efference copy models of song control (17), but more specific predictions are needed to validate these models.

The social context in which the birds sing may also influence the presence or absence of an error signal in LMAN. Zebra finches sing two song types that, although nearly identical in structure (25), are not generated by the same physiological mechanisms (37, 38). It has been suggested that when zebra finches sing to themselves or another male (undirected song) they are practicing and the error-correction process is turned on, whereas when they engage in courtship singing to a female (directed song) the error-correction process and LMAN are turned off (37). However, the current study clearly demonstrates that LMAN is "on" and generating precise spike patterns during directed singing. The current study was based on directed song because it can be elicited with the presentation of a female bird and is therefore more amenable to chronic recording in which LMAN neurons may be held for a limited time. Furthermore, LMAN spike patterns are much more precise during directed song than during undirected song (38), increasing the reliability of statistical analyses with limited sample sizes. Future work confirming the hypothesis that song error correction occurs primarily during undirected song would necessitate repeating these studies in the more difficult undirected song preparation.

This study provides the first measurements of single-neuron LMAN activity in zebra finches singing with normal and altered auditory feedback. The results cast doubt on the role of BOS-tuned LMAN neurons as real-time error detectors and lend support to the notion that a motor signal, rather than an auditory one, drives LMAN neurons during song production. The combination of motor inputs to LMAN in the singing bird and auditory inputs to LMAN in the anesthetized bird highlights the multimodal nature of this nucleus. Likewise, auditory responses are well known in the nuclei of the motor pathway in the anesthetized bird (39, 40) and the sleeping bird (41). Although it has been convenient to think of these pathways as strictly motor or auditory in function (Fig. 1), such is clearly not the case in practice. The prevalence of such multimodal processing indicates that it is a major design feature of the song control system that has thus far eluded explanation and should be a considerable focus of future research.

I thank M. Konishi, in whose laboratory this work was done, for valuable discussions and R. Egnor and A. Doupe for comments on an earlier version of the manuscript. This work was supported, in part, by National Institutes of Health Grant MH55984 (to M. Konishi).

1. Houde, J. F. & Jordan, M. I. (1998) *Science* **279,** 1213–1216.
2. Konishi, M. (1965) *Z. Tierpsychol.* **22,** 770–783.
3. Nordeen, K. & Nordeen, E. (1992) *Behav. Neural Biol.* **57,** 58–66.
4. Okanoya, K. & Yamaguchi, A. (1997) *J. Neurobiol.* **33,** 343–356.
5. Wooley, S. & Rubel, E. (1997) *J. Neurosci.* **17,** 6380–6390.
6. Nottebohm, F., Stokes, T. & Leonard, C. (1976) *J. Comp. Neurol.* **165,** 457–486.
7. Bottjer, S. W., Halsema, K. A., Brown, S. A. & Miesner, E. A. (1989) *J. Comp. Neurol.* **279,** 312–326.
8. Reiner, A., Perkel, D., Bruce, L., Butler, A., Csillag, A., Kuenzel, W., Medina, L., Paxinos, G., Shimizu, T., Streidter, G., *et al*. (2004) *J. Comp. Neurol.* **473,** 377–414.
9. Scharff, C. & Nottebohm, F. (1991) *J. Neurosci.* **11,** 2896–2913.
10. Basham, M. E., Nordeen, E. & Nordeen, K. (1996) *Neurobiol. Learn. Mem.* **66,** 295–302.
11. Brainard, M. & Doupe, A. (2000) *Nature* **404,** 762–766.
12. Brainard, M. & Doupe, A. (2000) *Nat. Rev. Neurosci.* **1,** 31–40.
13. Doupe, A. & Konishi, M. (1991) *Proc. Natl. Acad. Sci. USA* **88,** 11339–11343.
14. Doupe, A. J. (1997) *J. Neurosci.* **17,** 1147–1167.
15. Solis, M. & Doupe, A. (2000) *Neuron* **25,** 109–121.
16. Rosen, M. & Mooney, R. (2000) *J. Neurosci.* **20,** 5437–5488.
17. Troyer, T. W. & Doupe, A. J. (2000) *J. Neurophysiol.* **84,** 1204–1223.
18. Dave, A. S. & Margoliash, D. (2000) *Science* **290,** 812–816.
19. Margoliash, D. (2000) *J. Comp. Physiol. A* **188,** 851–866.
20. Leonardo, A. & Konishi, M. (1999) *Nature* **399,** 466–470.
21. Lombardino, A. J. & Nottebohm, F. (2000) *J. Neurosci.* **20,** 5054–5064.
22. Fee, M. S. & Leonardo, A. (2001) *J. Neurosci. Methods* **112,** 83–94.
23. Hessler, N. & Doupe, A. (1999) *J. Neurosci.* **19,** 10461–10481.
24. Livingston, F. & Mooney, R. (1997) *J. Neurosci.* **12,** 8997–9009.
25. Sossinka, R. & Bohner, J. (1980) *Z. Tierpsychol.* **53,** 123–132.
26. Wooley, S. & Rubel, E. (1999) *J. Neurosci.* **19,** 358–371.
27. Zevin, J., Seidenberg, M. & Bottjer, S. (2004) *J. Neurosci.* **24,** 5849–5862.
28. Foster, S. (1986) in *IEEE International Conference on Acoustics, Speech, and Signal Processing* (Tokyo), pp. 929–932.
29. Zhou, G., Green, D. & Middlebrooks, J. (1992) *J. Acoust. Soc. Am.* **92,** 1169–1171.
30. Golay, M. (1961) *IRE Trans. Inform. Theory* **2,** 82–87.
31. Thomson, D. (1982) *Proc. IEEE* **70,** 1055–1096.
32. Tchernichovski, O., Nottebohm, F., Ho, C., Pesaran, B. & Mitra, P. (2000) *Anim. Behav.* **59,** 1167–1176.
33. Leonardo, A. (2002) Ph.D. thesis (California Institute of Technology, Pasadena).
34. Solis, M. & Doupe, A. (1999) *J. Neurosci.* **19,** 4559–4584.
35. Zar, J. (1999) *Biostatistical Analysis* (Prentice–Hall, Upper Saddle River, NJ).
36. Chi, Z. & Margoliash, D. (2001) *Neuron* **32,** 899–910.
37. Jarvis, E., Scharff, C., Grossman, M., Ramos, J. & Nottebohm, F. (1998) *Neuron* **21,** 775–788.
38. Hessler, N. & Doupe, A. (1999) *Nat. Neurosci.* **2,** 209–211.
39. Vicario, D. & Yohay, K. (1993) *J. Neurobiol.* **24,** 488–505.
40. Williams, H. & Nottebohm, F. (1985) *Science* **229,** 279–282.
41. Dave, A. S., Yu, A. C. & Margoliash, D. (1998) *Science* **282,** 2250–2254.